Hindawi
Shock and Vibration
Volume 2019, Article ID 3702919, 14 pages
https://doi.org/10.1155/2019/3702919

Research Article

Integrated Vibration Control of In-Wheel Motor-Suspensions Coupling System via Dynamics Parameter Optimization

Wei Wang,[1] **Mu Niu**,[1] **and Yuling Song**[1,2,3]

[1]*College of Mechanical and Electronic Engineering, Northwest A&F University, Yangling, Shaanxi 712100, China*
[2]*Key Laboratory of Agricultural Internet of Things, Ministry of Agriculture and Rural Affairs, Yangling, Shaanxi 712100, China*
[3]*Shaanxi Key Laboratory of Agricultural Information Perception and Intelligent Services, Yangling, Shaanxi 712100, China*

Correspondence should be addressed to Yuling Song; syl791026@126.com

Received 6 February 2019; Revised 28 March 2019; Accepted 2 May 2019; Published 28 August 2019

Academic Editor: Adam Glowacz

In order to integrally control the vibration of in-wheel motor- (IWM-) suspensions coupling system of an electric vehicle, a novel nonlinear dynamics model of the coupling system, which consists of the motor magnetic gap (MMG), is established. Synthesizing subtargets of the vertical vibration acceleration of bodywork, the vertical deformation of tire, the suspension travel, and the vertical fluctuation of MMG, a composite optimization mathematical model is set up. Based on artificial fish swarm algorithm (AFSA), a novel dynamics parameter optimization method is proposed to search the optimal parameter combination existing in the nonlinear dynamics model. Simulation analyses demonstrate that the proposed optimization method is superior to genetic algorithm (GA) under the same optimization conditions, and it can significantly decrease the fluctuation of MMG and improve ride comfort.

1. Introduction

With the increase of energy crisis and environmental pollution, it has become an important research goal to develop zero emissions of electric vehicles (EVs). Among them, the IWM-driven EVs have received a general attention due to their advantages of simple vehicle layout, high integrated characteristic, flexible drive feature, and so on.

However, this kind of driven form also brings new vibration problems that need to be solved. In practice, the MMG of IWM generates fluctuation under road excitation. Electromagnetic force is a function of MMG [1–3], for which the changes of electromagnetic force caused by the fluctuation of MMG deteriorate the ride comfort of an electric wheel vehicle [4, 5]. Furthermore, because the outer rotor of IWM is fixed on a hub, the fluctuation of MMG affects the adhesion performance between tire and ground [6]. In addition, motor, brake, and other components are highly integrated in a wheel which makes the unsprung mass increase and leads to poor dynamics behaviors [6]. In view of the reasons mentioned above, some research studies have been done to reduce the vibration of electric wheel vehicle. An advanced dynamics damping motor system was proposed by Shao et al. [7], which isolates the IWM vibration by an in-wheel spring damping element that has internal damping effect. This structural form breaks through the concept of traditional suspension system and provides theoretical support for the improvement of suspension structure. Except for changing systematic structure, Pang et al. [8] argued that it is also one of the most effective ways to adjust dynamics parameters for improving the performance of suspension system. The experimental results from a quarter car test rig which were done by Mitra et al. [9] show that mass and damping coefficient are the most influential parameters for ride comfort. Therefore, many scholars focus their attention on optimizing the mass, damping coefficient, and stiffness coefficient of suspension system and achieve many significant results in enhancing ride comfort by using GA [10–14]. Essentially, the dynamics parameter optimization of suspension system belongs to a multiobjective optimization problem (MOOP) which can be solved by using multiobjective optimization algorithm (MOOA) [15, 16]. Gadhvi et al. [15], respectively, used nondominated sorting genetic algorithm (NSGA), strength Pareto evolutionary algorithm (SPEA), and Pareto envelope-based selection algorithm (PESA) as tools for suspension optimization. It is proved that the results of the three MOOAs

are different from each other in optimization effect. Thus, an appropriate MOOA plays an important role in solving MOOPs. The behaviors and evolutions of natural creatures bring enlightenments to practical optimization problems [17, 18]. Recently, the AFSA has been quickly developed. The main behavior of fish used by the AFSA is fish stay near their swarm to protect themselves from predators and meanwhile maintain safe distances from nearby partners to search food without collisions [19]. The basic idea of AFSA adopted by He et al. [20] is partly derived from the aforementioned fish behaviors. The AFSA has been successfully applied to many different fields, such as the scheduling of renewable energy sources in a microgrid [21], a multiobjective fuzzy disassembly balancing problem [22], and dynamic weapon target assignment problem [23] because of its advantages of parallelism, global feature, traceability, and so on. Since the AFSA has a good ability to solve the above MOOP problems, it is a viable means to optimize the key dynamics parameters of the IWM-suspensions coupling system based on the AFSA.

To sum up, the chassis structure of IWM-driven EV is different from that of traditional vehicle, for which some researchers have designed new in-wheel spring-damping elements to reduce control vibration of the chassis and improve the ride comfort. In addition to this method, other researches mainly focus on the vibration reduction of suspension system by using advanced optimization methods and different control methods. Although the influences of dynamics parameters on suspension system are revealed and the developments of optimization methods provide new ways for improving ride comfort, the research on the dynamics parameter optimization of IWM-suspensions coupling system is insufficient, and the dynamics parameters of IWM are usually overlooked, which is an obstacle to the integrated vibration control of IWM-suspensions coupling system and brings about unreasonable dynamics parameter combinations. This is an important problem that needs to be urgently resolved.

In this research, synthetically considering the dynamics parameters of IWM-suspensions coupling system, a novel nonlinear dynamics model, which consists of the MMG, is established. Based on the AFSA, a novel dynamics parameter optimization method is proposed by constructing optimization mathematical model and constraints. Eight key dynamics parameters of the IWM-suspensions coupling system are optimized, and the optimal parameter combination is obtained. The vibration control effect of the proposed method is numerically validated by comparing to GA's optimization results under different road excitations. The optimization method proposed by this paper has important application prospects in the field of vehicular multisystem integrated dynamics design and control, e.g., the integrated design and control of electric wheel-steering-suspension system.

2. Model and Problem Formulation

2.1. Dynamics Modeling. The motor bearing that supports the rim is subjected to circumferential, radial, and axial forces which results in the relative displacement between the stator and the rotor, and the fluctuation of MMG further deteriorates the vibration of vehicle. In this part, the fluctuation of MMG caused by road excitation is mainly considered, and the incentive role of torque fluctuation produced by motor structure, processing error, and principle factor is neglected because it is far less than the road excitation [5]. According to the actual structure of IWM-suspensions coupling system described in Figure 1, a quarter-car nonlinear vibration model is established and shown in Figure 2. Different from the traditional one, this nonlinear IWM-suspensions coupling system uses a suspension element to elastically isolate the overall IWM mass from unsprung mass (see Figure 1).

Currently, nonlinear components are widely applied to vehicle systems because of their predominant damping performances. Most vehicles universally use nonlinear suspensions and tires to reduce their vertical vibrations. Therefore, the nonlinear stiffness characteristics of the suspension 1 and tire are taken into account. The elastic restoring forces models of suspension 1 and the tire are, respectively, expressed as [24]

$$F_s = k_s \cdot x_s \cdot \left(1 + \varepsilon \cdot x_s^2\right), \tag{1}$$

$$F_t = k_t \cdot x_t \cdot \left(1 + \gamma \cdot x_t^2\right), \tag{2}$$

where F_s and F_t, respectively, represent the vertical elastic restoring forces of suspension 1 and the tire. k_s and k_t are, respectively, the stiffness coefficients of suspension 1 and the tire. x_s and x_t are respective vertical deformations of suspension 1 and the tire. ε and γ are nonlinearity coefficients.

Based on formulae (1) and (2), referring to the quarter-car nonlinear vibration model shown in Figure 2, the motion equation of IWM/suspensions coupling system is written as follows:

$$\begin{cases} m_1\ddot{y}_1 + c_1(\dot{y}_1 - \dot{y}_0) + c_2(\dot{y}_1 - \dot{y}_2) + c_7(\dot{y}_1 - \dot{y}_5) + k_1(y_1 - y_0) + \gamma \cdot k_1(y_1 - y_0)^3 + k_2(y_1 - y_2) + k_7(y_1 - y_5) = 0, \\ m_2\ddot{y}_2 + c_2(\dot{y}_2 - \dot{y}_1) + c_3(\dot{y}_2 - \dot{y}_3) + c_6(\dot{y}_2 - \dot{y}_4) + k_2(y_2 - y_1) + k_3(y_2 - y_3) + \varepsilon \cdot k_3(y_2 - y_3)^3 + k_6(y_2 - y_4) = 0, \\ m_3\ddot{y}_3 + c_3(\dot{y}_3 - \dot{y}_2) + c_4(\dot{y}_3 - \dot{y}_4) + k_3(y_3 - y_2) + \varepsilon \cdot k_3(y_3 - y_2)^3 + k_4(y_3 - y_4) = 0, \\ m_4\ddot{y}_4 + c_4(\dot{y}_4 - \dot{y}_3) + c_5(\dot{y}_4 - \dot{y}_5) + c_6(\dot{y}_4 - \dot{y}_2) + k_4(y_4 - y_3) + k_5(y_4 - y_5) + k_6(y_4 - y_2) = 0, \\ m_5\ddot{y}_5 + c_5(\dot{y}_5 - \dot{y}_4) + c_7(\dot{y}_5 - \dot{y}_1) + k_5(y_5 - y_4) + k_7(y_5 - y_1) = 0, \end{cases} \tag{3}$$

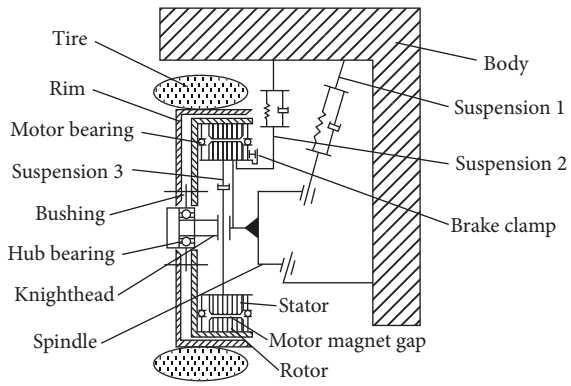

Figure 1: The structure of IWM-suspensions coupling system.

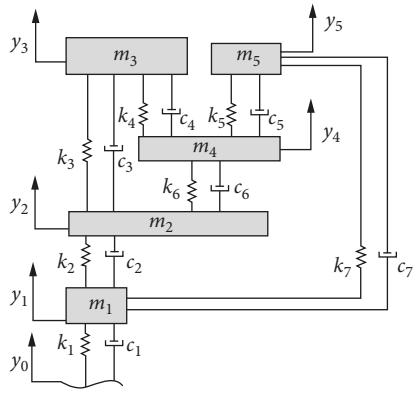

Figure 2: The quarter-car nonlinear vibration model.

where m_1 denotes the total mass of the tire and rim. m_2 is the total mass of the knighthead and brake clamp. m_3 is the mass of the quarter bodywork. m_4 and m_5, respectively, denote the mass of IWM's stator and rotor. y_0 is harmonic road excitation. y_1, y_2, y_3, y_4, and y_5, respectively, represent the vertical displacements of m_1, m_2, m_3, m_4, and m_5. k_1 and c_1, respectively, denote the vertical stiffness and damping coefficients of the tire. k_2 and c_2, respectively, denote the vertical stiffness and damping coefficients of hub bearing. k_3 and c_3, respectively, denote the equivalent vertical stiffness and damping coefficients of suspension 1 (see Figure 1). k_4 and c_4, respectively, denote the stiffness and damping coefficients of suspension 2 between motor stator and bodywork. k_5 and c_5, respectively, represent the stiffness and damping coefficients of the bearing between motor stator and rotor. k_6 and c_6, respectively, are the stiffness and damping coefficients of suspension 3 between motor stator and knighthead. k_7 and c_7, respectively, denote the vertical stiffness and damping coefficients of the bushing between the motor rotor and the rim.

2.2. Model and Method of Optimization. The AFSA has a good ability to overcome local extreme value and obtain global optimal solution in search space [19]. Here, in accordance with the experimental results by Mitra et al. [9]; eight key dynamics parameters of IWM-suspensions coupling system are chosen as design variables. They are m_1, m_3, k_3, k_4, k_6, c_3, c_4, and c_6, respectively.

2.2.1. Mathematical Model of Optimization. Ride comfort is an important consideration in the design of vehicular suspension system, particularly the performance evaluation indices of vehicular suspension system [25, 26]. Traditional evaluation indices, such as the vertical vibration acceleration of bodywork, the vertical deformation of tire, and suspension travel, can influence the ride comfort of a vehicle. However, the fluctuation of IWM's MMG is neglected which can deteriorate the ride comfort. So, here the fluctuation of IWM's MMG is added to the indices.

Weighted-sum method is used to indicate the importance of each index and connect subtargets into a composite optimization objective. Root-mean-square (RMS) value is used to reduce the impact of contingency factors. The mathematical model of optimization problem is written as

$$F(f) = \min\left\{\frac{1}{\int_{t_1}^{t_2}\left[\left(\lambda_1 f_1^2/\mathrm{RMS}\left(f_1^2\right)\right)+\left(\lambda_2 f_2^2/\mathrm{RMS}\left(f_2^2\right)\right)+\left(\lambda_3 f_3^2/\mathrm{RMS}\left(f_3^2\right)\right)+\left(\lambda_4 f_4^2/\mathrm{RMS}\left(f_4^2\right)\right)\right]dt}\right\}, \quad (4)$$

subject to

$$\begin{cases} g_1 = l_1 - |y_2 - y_3| \geq 0, \\ g_2 = l_2 - |y_4 - y_5| \geq 0, \\ 45\,(\text{kg}) \leq m_1 \leq 60\,(\text{kg}), \\ 310\,(\text{kg}) \leq m_3 \leq 350\,(\text{kg}), \\ 10\,(\text{kN/m}) \leq k_3 \leq 80\,(\text{kN/m}), \\ 10\,(\text{kN/m}) \leq k_4 \leq 30\,(\text{kN/m}), \\ 10\,(\text{kN/m}) \leq k_6 \leq 30\,(\text{kN/m}), \\ 200\,(\text{Ns/m}) \leq c_3 \leq 2000\,(\text{Ns/m}), \\ 100\,(\text{Ns/m}) \leq c_4 \leq 800\,(\text{Ns/m}), \\ 10000\,(\text{Ns/m}) \leq c_6 \leq 35000\,(\text{Ns/m}), \end{cases} \tag{5}$$

where $f_1 = \ddot{y}_3$, $f_2 = (y_1 - y_0)$, $f_3 = (y_3 - y_2)$, and $f_4 = (y_5 - y_4)$ which, respectively, denote the vertical vibration acceleration of bodywork, the vertical deformation of tire, the suspension travel, and the vertical fluctuation of IWM's MMG. $F(f)$ is an objective function. $t_1 = 0$ s, $t_2 = 10$ s; this time period includes the transient and steady-state response of dynamics system. λ_1, λ_2, λ_3, and λ_4 are, respectively, the weighted value of each performance index which are assigned to be 0.25, 0.2, 0.2, and 0.35. g_1 and g_2 are constraints. $l_1 = 9$ cm and $l_2 = 0.5$ mm, respectively, denote the suspension limit travel and the limit value of MMG.

2.2.2. AFSA-Based Optimization Method and Procedure. The number of artificial fishes (AFs) in fish swarm is defined as N and each AF that includes the 8 dynamics parameters (i.e., $m_1, m_3, k_3, k_4, k_6, c_3, c_4$, and c_6) is denoted by $\mathbf{AF}_i (i = 1, 2, \ldots, N)$. So, $\mathbf{AF}_i$ can be written as $\mathbf{AF}_i = [x_{1i}, x_{2i}, \ldots, x_{8i}]^T$, where each element in the vector represents a dynamics parameter. In this way, the fish swarm can be expressed by an $8 \times N$ matrix which is shown in Figure 3. Each column of the matrix represents an artificial fish and its position.

By substituting $\mathbf{AF}_i$ into formula (4), the corresponding $Y_i = F(f)$ can be obtained which is regarded as food concentration in the current position (also means the fitness in GA). As shown in Figure 4, *Step* is the AF's movement size, *Visual* is AF's field of view. *Try-number* is defined as the maximum number of attempts of foraging behavior. To avoid overcrowding with the surrounding partners, a congestion factor delta is set up which is expressed as follows:

$$\text{delta} = \frac{1}{\alpha \cdot n_{\text{limit}}}, \tag{6}$$

where α represents the degree of approximation of extremes and it is a coefficient between 0 and 1. n_{limit} is the maximum upper limit of the AF's number existing in the field of view. Here we choose $\alpha = 0.9$ and $n_{\text{limit}} = 2$.

The initial data of each AF in artificial fish swarm must be defined in advance which can be randomly generated within their definition domains [10, 27]. Without losing of generality, the i-th AF is denoted as $\mathbf{AF}_i = [m_{1i}, m_{3i}, k_{3i}, k_{4i}, k_{6i}, c_{3i}, c_{4i}, c_{6i}]^T$. After initializing

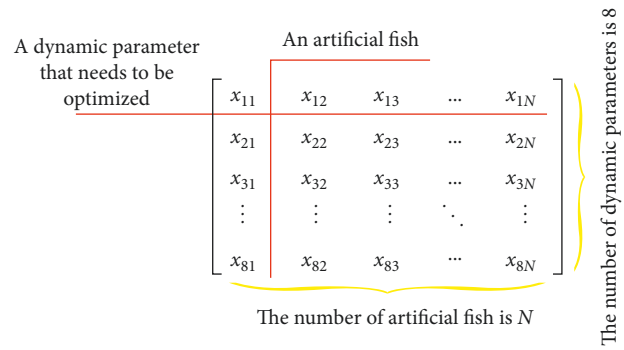

Figure 3: The expression of artificial fish swarm.

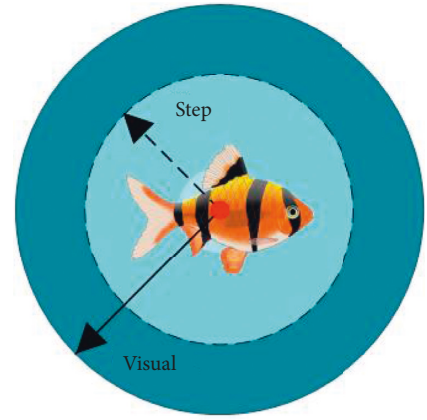

Figure 4: AF's visual and moving step.

an artificial fish swarm, the AFs in the fish swarm search the optimal solution by iterations. During each iteration, the AFs update themselves by the following steps.

(1) Random Moving Behavior and Foraging Behavior. Random moving behavior is a kind of default foraging behavior during which $\mathbf{AF}_i$ randomly selects a state $\mathbf{AF}_j$ within its *visual* (formula (7)) and then moves one *step* to a new position $\mathbf{AF}_{\text{next}}$ (formula (8)). In the foraging behavior, the AF always tries to move to a better place based on the food concentration, which lays the foundation of convergence.

$$\mathbf{AF}_j = [m_{1i}, m_{3i}, k_{3i}, k_{4i}, k_{6i}, c_{3i}, c_{4i}, c_{6i}]^T + \text{visual} \times (a_{mn})_{8\times 1}, \tag{7}$$

where a_{mn} is an uniformly distributed random number over the interval $[-1, 1]$ and $a_{mn} \neq 0$.

$$\mathbf{AF}_{\text{next}} = [m_{1i}, m_{3i}, k_{3i}, k_{4i}, k_{6i}, c_{3i}, c_{4i}, c_{6i}]^T + \beta \times \text{step} \times \frac{\mathbf{AF}_j - \mathbf{AF}_i}{\left\|\mathbf{AF}_j - \mathbf{AF}_i\right\|}, \tag{8}$$

where $\beta = \min(|\alpha_{mn}|)$ (Pseudocode 1).

(2) Swarm Behavior. This behavior enables $\mathbf{AF}_i$ to move as much as possible to the center of nearby partners $\mathbf{AF}_{\text{center}}$

```
for 1 to try-number;
randomly select a new position (formula (7));
   if beyond the definition domain;
      select boundary value;
   if the food concentration of the new position is higher;
      move a step to the next position (formula (8));
      break.
end.
if foraging behavior fails;
   randomly select a position;
end.
```

Pseudocode 1

and avoid egregious overcrowding. The center of nearby partners is given by

$$\mathbf{AF}_{\text{center}} = \frac{\sum_{j+1}^{n_f} \mathbf{AF}_j}{n_f}, \tag{9}$$

where n_f is the number of nearby partners that is calculated by using the formula $\|\mathbf{AF}_j - \mathbf{AF}_i\| \le \text{visual}$. The criteria for judging congestion are given by formula (10), which decides whether to follow formula (11).

$$\frac{Y_{\text{center}}}{Y_i \cdot n_f} > \text{delta}, \tag{10}$$

where Y_{center} represents the food concentration of $\mathbf{AF}_{\text{center}}$.

$$\mathbf{AF}_{\text{next}} = [m_{1i}, m_{3i}, k_{3i}, k_{4i}, k_{6i}, c_{3i}, c_{4i}, c_{6i}]^T + \text{rand}() \times \text{step} \times \frac{\mathbf{AF}_{\text{center}} - \mathbf{AF}_i}{\left\|\mathbf{AF}_{\text{center}} - \mathbf{AF}_i\right\|}, \tag{11}$$

where rand() is an random number over the interval (0, 1) (Pseudocode 2).

(3) Following Behavior. $\mathbf{AF}_i$ searches for partners within its *visual* and selectively moves to the one with the highest food concentration. If formula (12) is satisfied, $\mathbf{AF}_i$ moves according to formula (13):

$$\frac{Y_{\max}}{Y_i \cdot n_f} > \text{delta}, \tag{12}$$

$$\mathbf{AF}_{\text{next}} = [m_{1i}, m_{3i}, k_{3i}, k_{4i}, k_{6i}, c_{3i}, c_{4i}, c_{6i}]^T + \text{rand}() \times \text{step} \times \frac{\mathbf{AF}_{\max} - \mathbf{AF}_i}{\left\|\mathbf{AF}_{\max} - \mathbf{AF}_i\right\|}, \tag{13}$$

where $\mathbf{AF}_{\max}$ is the AF with the highest food concentration $Y_{\max}$ (Pseudocode 3).

The dynamics parameter optimization procedure of nonlinear IWM-suspensions coupling system is shown in Figure 5.

3. Optimization Results

The overall dynamics parameter optimization procedure is executed by Matlab software. In order to easily choose *Step* and *Visual* and accelerate convergence, during the optimization process, all the design variables are reduced to two digits and then the optimization results are zoomed out to the same multiple. The GA-based multiparameter optimization scheme is used for comparison with the proposed optimization method, which includes coding, crossing, mutation, and selecting operations [10]. Road excitation is simulated by the harmonic function described in formula (15).

(1) The parameters involved in the proposed optimization method are set up as below:

(i) Number of AF: 15
(ii) Max iteration: 1000
(iii) Step: 0.5
(iv) Visual: 5
(v) Try-number: 3
(vi) Delta: 0.5556

(2) The selected optimization conditions for GA:

(i) Number of individuals: 15
(ii) Max iteration: 1000
(iii) Crossover rate: 0.9
(iv) Mutation rate: 0.5
(v) Selecting rate: 0.8

For the established motion equation of nonlinear IWM-suspensions coupling system, the nonlinear coefficients γ and ε are both assigned to be 0.5. The dynamics parameter optimization results are shown in Table 1, where the original dynamics parameters of nonlinear IWM-suspensions coupling system are listed [28].

The larger the fish swarm, the greater the ability to jump out from the local extreme value and the faster the convergence rate, but the amount of each iteration calculation is also greater. Numerical experiments show that when the number of AF is 15, the amount of calculation and the convergence rate reach a good balance. The changes of food concentration calculated by the proposed method are shown in Figure 6. It can be seen that the food concentration increases from 5.693×10^{-3} to 6.491×10^{-3} step by step within 1000 iterations. From the whole optimization procedure, the food concentration breaks though local extreme values for four times and eventually reaches a global extreme value. This phenomenon interprets the global convergence characteristic of the proposed optimization method. The iteration process of each parameter is shown in Figures 7(a)–7(h) from which it is easy to see that c_3 achieves convergence faster than other parameters. c_3 and c_4 finally converge to the boundaries of their definition domains.

4. Simulation Analyses of Optimization Control Effects

In this Section, numerical simulations are executed to compare and verify the optimization control effects of the proposed method and GA. Rough and bump road excitations simulated by harmonic functions [2] are used to

```
search for partners within the visual;
if found partners;
   obtain the center position (formula (9)) and the corresponding food concentration;
   if the position has higher food concentration (Y_center > Y_i) and not very crowded (formula (10));
      move to the position (formula (11));
   else
      foraging behavior;
   end.
else
   foraging behavior;
end.
```

Pseudocode 2

```
search for partners within the visual;
if found partners;
   obtain the position of the AF who owns the maximum food concentration;
   if its food concentration is higher (Y_max > Y_i) and not very crowded (formula (12));
     move to the position (formula (13));
   else
      foraging behavior;
   end.
else
   foraging behavior;
end.
```

Pseudocode 3

evaluate dynamic performances of the nonlinear IWM-suspensions coupling system by analyzing the vertical vibration acceleration of bodywork, bodywork travel, tire dynamic load, suspension travel (y_3–y_2), and the MMG of IWM. The parameters involved in simulations are listed in Table 1.

4.1. Response Analyses under Rough Road Excitation. The function of rough road profile in time domain can be expressed as follows:

$$y_0(t) = \frac{a}{2}\left[\cos\left(\frac{2\pi V_0}{l}t\right) - 1\right], \quad t \geq 0, \tag{14}$$

where $a = 0.1$ m and $l = 15$ m. They, respectively, denote depth and length of the rough road profile. The vehicle velocity is $V_0 = 60$ km/h.

From the data shown in Tables 2 and 3, it can be seen that although the both optimization methods can improve dynamic performances of the nonlinear coupling system, compared with the GA, the optimization control effect of the proposed method is more obvious. Under rough road excitation, the nonlinear coupling system with the dynamics parameters optimized by the proposed method has better dynamic indicators, especially the maximum IWM's MMG and the maximum suspension travel which are, respectively, decreased by 50% and 75%. Response comparisons of the nonlinear coupling system optimized by different methods are shown in Figures 8(a)–8(e).

Under rough road excitation and using different optimization methods, the bodywork vertical vibration acceleration, the bodywork travel, the suspension travel, the tire dynamic load, and the IWM's vertical MMG of nonlinear IWM-suspensions coupling systems are depicted in Figures 8(a)–8(e). It can be seen that the dynamic responses of the optimized nonlinear IWM-suspensions coupling system are improved and their amplitudes are reduced. The vibrations experienced by passengers in the vehicle are reduced with the decreases of bodywork vertical vibration acceleration and bodywork travel, and the ride comfort is meanwhile enhanced. The decreased vertical fluctuation of the MMG indicates that the relative displacement between the stator and the rotor changes smoothly, which reduces unbalanced electromagnetic force waves, decreases motor wear, and extends motor bearing life. Lower tire dynamic load can extend tire life and reduce the frequency of tire replacement. From Tables 2 and 3 and Figures 8(a)–8(e), it can also be clearly seen that although dynamic characteristics of the GA-optimized coupling system have been improved, the minimum value of all the response indicators is always obtained by the proposed method which indicates that the proposed AFSA-based method has better optimization control effects.

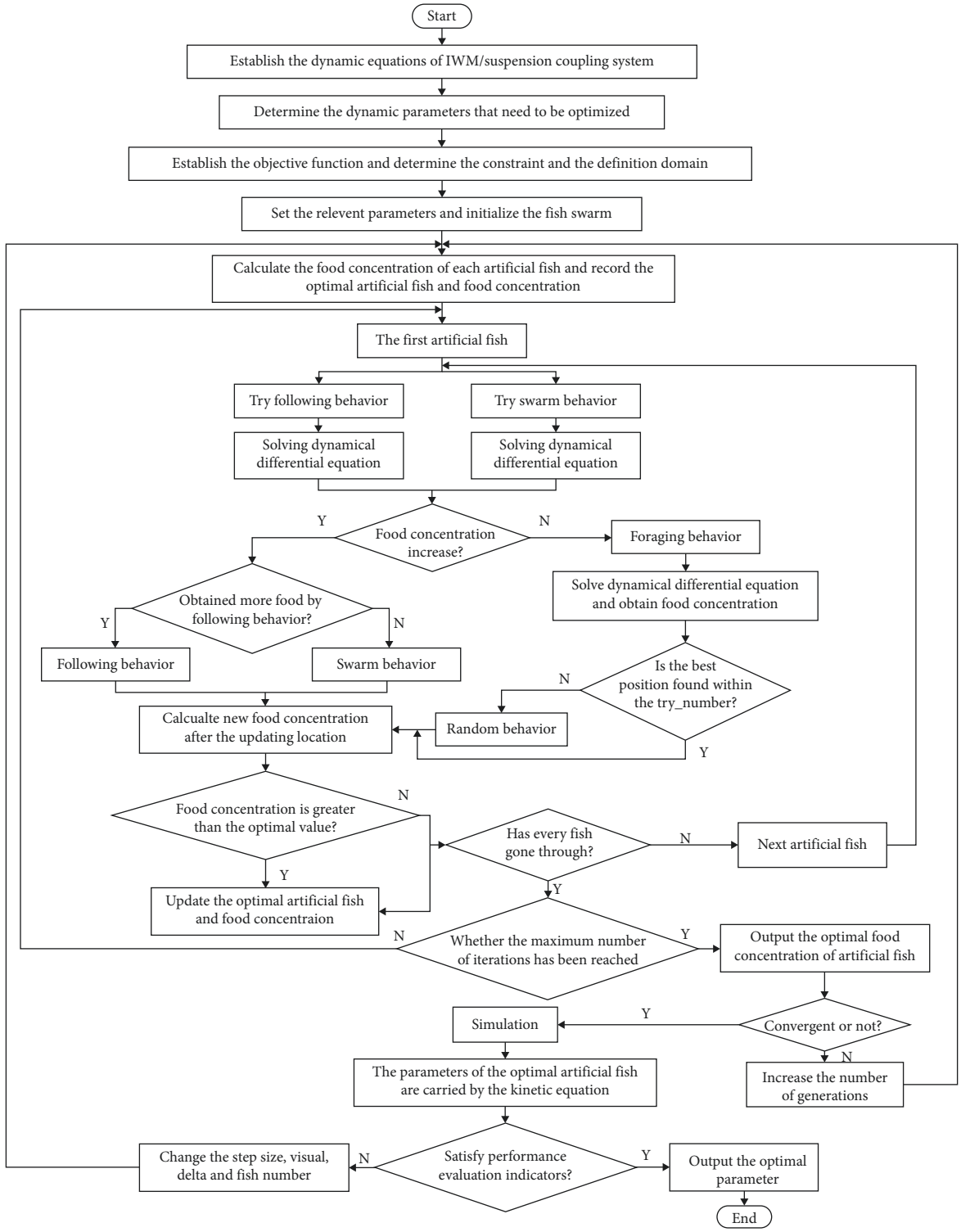

Figure 5: Dynamics parameter optimization procedure.

4.2. Response Analyses under Bump Road Excitation. Bump road excitation is adopted to analyze dynamic response characteristics of the nonlinear IWM-suspensions coupling system optimized by different methods, and its profile is described by the function below:

$$y_0(t) = \begin{cases} \dfrac{h}{2}\left(1 - \cos\left(\dfrac{2\pi V_0}{\lambda} t\right)\right), & 0 \le t \le \dfrac{\lambda}{V_0}, \\ 0, & t \ge \dfrac{\lambda}{V_0}, \end{cases} \tag{15}$$

Table 1: The dynamics parameter optimization results.

Parameters	Original values	Optimal values (by the proposed method)	Optimal values (by GA)	Units
m_1	60	58.7964	56.0428	kg
m_2	5	—	—	kg
m_3	327	328.3650	347.2638	kg
m_4	18	—	—	kg
m_5	12	—	—	kg
k_1	250000	—	—	N/m
k_2	5120000	—	—	N/m
k_3	25000	78246.5801	25983.2784	N/m
k_4	15000	27137.5320	26064.2881	N/m
k_5	5000000	—	—	N/m
k_6	10000	14215.9274	26016.6510	N/m
k_7	150000	—	—	N/m
c_1	375	—	—	N·s/m
c_2	10	—	—	N·s/m
c_3	800	2000.0000	1911.8151	N·s/m
c_4	100	800.0000	623.2551	N·s/m
c_5	10	—	—	N·s/m
c_6	15000	12825.0224	17197.6337	N·s/m
c_7	450	—	—	N·s/m

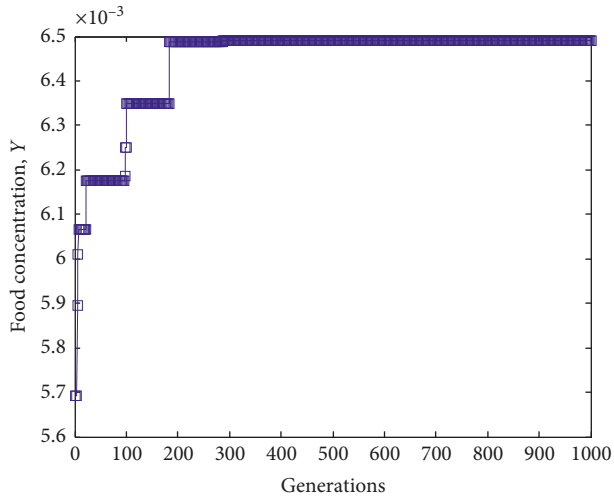

Figure 6: The iteration process of food concentration.

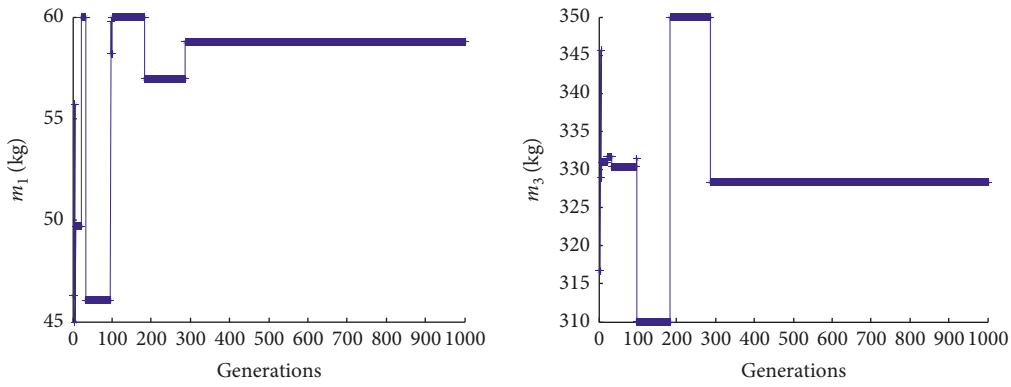

Figure 7: Continued.

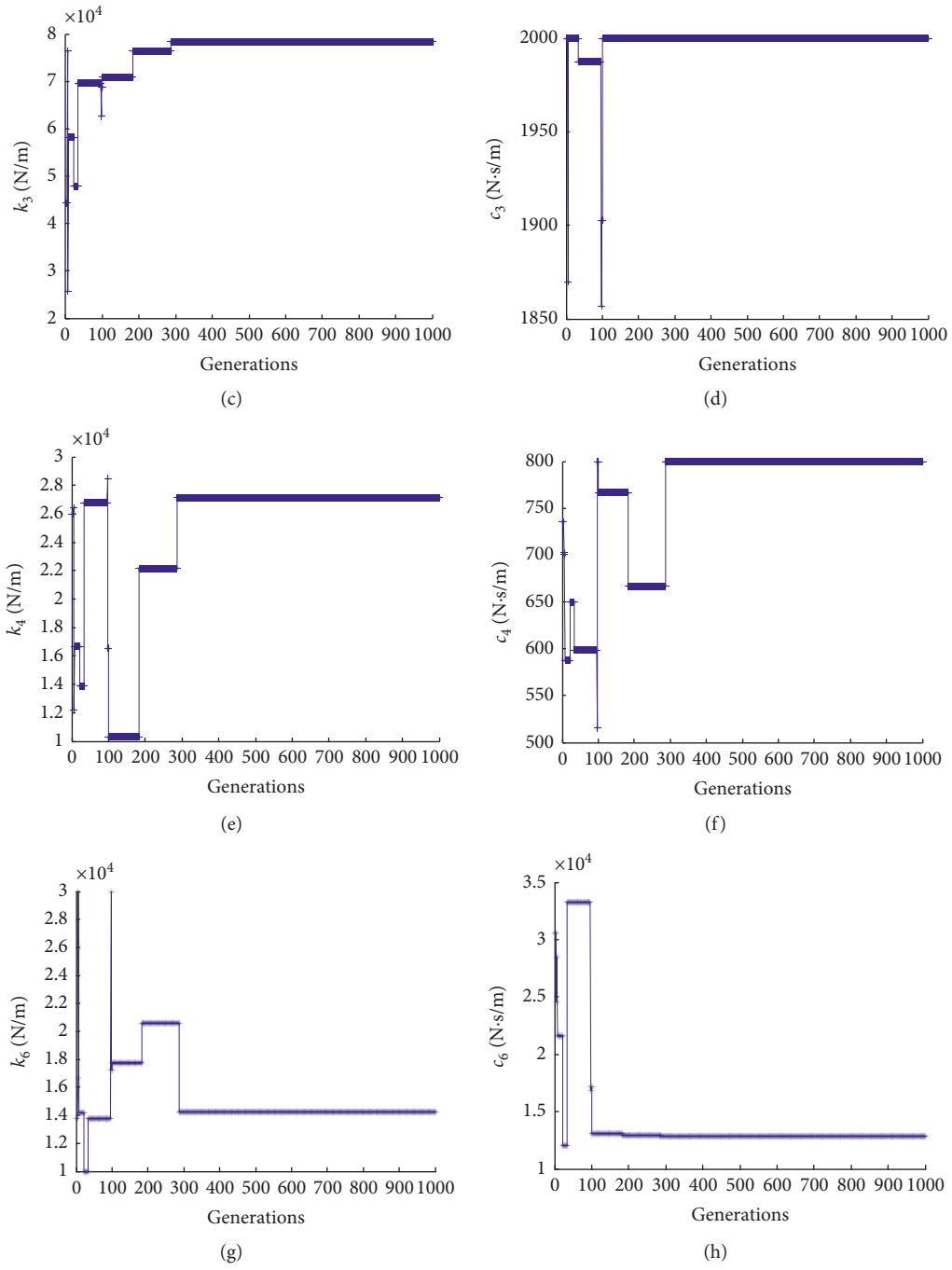

Figure 7: The iteration process of each dynamics parameter. (a) Optimization iteration of m_1. (b) Optimization iteration of m_3. (c) Optimization iteration of k_3. (d) Optimization iteration of c_3. (e) Optimization iteration of k_4. (f) Optimization iteration of c_4. (g) Optimization iteration of k_6. (h) Optimization iteration of c_6.

where h and λ, respectively, denote height and length of the bump road profile. Here we choose $h = 0.1$ m, $\lambda = 5$ m, and the vehicle velocity $V_0 = 25$ km/h.

Tables 4 and 5, respectively, give the computation results of response indicators of the nonlinear coupling system optimized by different methods and the descending percentages of some important indicators from which it can be clearly confirmed that the nonlinear coupling system optimized by the proposed method achieves the maximum descending percentages of response indicators compared with the GA-optimized one. The maximum values of bodywork acceleration, bodywork travel, tire dynamic load, suspension travel, and IWM's MMG are individually reduced by 28%, 18%, 39%, 74%, and 53%, which indicates that the nonlinear coupling system optimized by the proposed method has better dynamic performance under bump road excitation. The response comparisons of the nonlinear IWM-suspensions coupling system optimized by different methods are shown in Figures 9(a)–9(e).

Table 2: The comparisons of response indicators calculated by using different dynamic parameters.

Indexes	The maximum value of the bodywork acceleration (m/s^2)	The maximum value of the bodywork travel (m)	The maximum value of the suspension travel (m)	The maximum value of the tire dynamic load (N)	The maximum value of the IWM's MMG (mm)	RMS of IWM's MMG (mm)	RMS of the bodywork acceleration (m/s^2)
Using original parameters	6.39	0.153	0.055	2426	0.12	0.066	3.581
Using parameters optimized by the GA	4.54	0.134	0.029	1834	0.10	0.061	2.782
Using parameters optimized by the proposed method	4.44	0.121	0.014	1799	0.06	0.032	2.332

Table 3: The descending percentages of the response indicators compared with original system.

Indexes	The descending percentage of the maximum bodywork acceleration (%)	The descending percentage of the maximum bodywork travel (%)	The descending percentage of the maximum suspension travel (%)	The descending percentage of the maximum tire dynamic load (%)	The descending percentage of the maximum IWM's MMG (%)
Using parameters optimized by the GA	29	12	47	24	17
Using parameters optimized by the proposed method	31	21	75	26	50

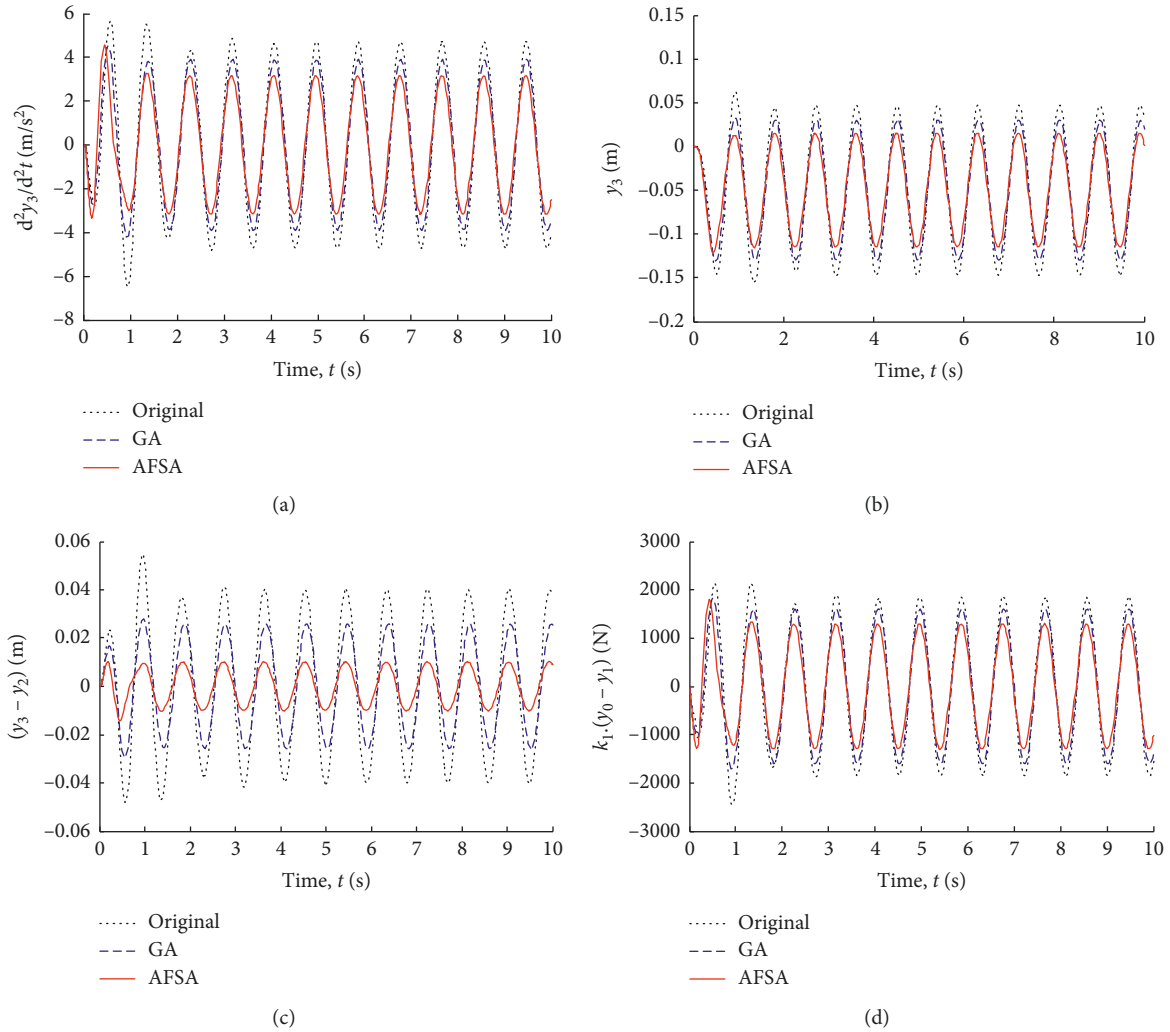

Figure 8: Continued.

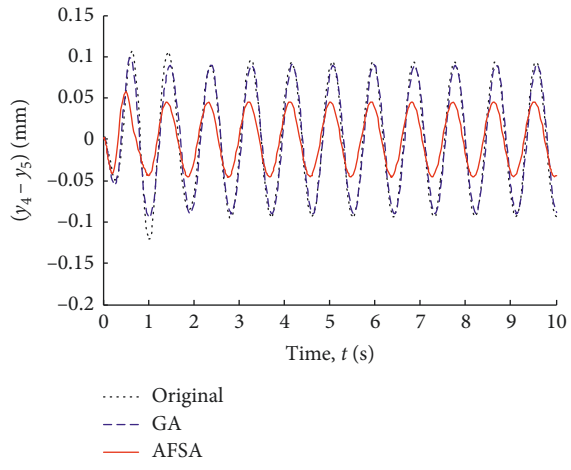

(e)

Figure 8: The response comparisons of the coupling system optimized by different methods. (a) The bodywork acceleration. (b) The bodywork travel. (c) The suspension travel. (d) The tire dynamic load. (e) The vertical MMG.

Table 4: The comparisons of response indicators calculated by using different dynamic parameters.

Indexes	The maximum value of the bodywork acceleration (m/s^2)	The maximum value of the bodywork travel (m)	The maximum value of the suspension travel (m)	The maximum value of the tire dynamic load (N)	The maximum value of the IWM's MMG (mm)	RMS of IWM's MMG (mm)	RMS of the bodywork acceleration (m/s^2)
Using original parameters	4.55	0.140	0.039	1742	0.088	0.032	1.818
Using parameters optimized by the GA	3.53	0.126	0.024	1435	0.078	0.028	1.324
Using parameters optimized by the proposed method	3.28	0.115	0.010	1065	0.041	0.015	1.171

Table 5: The descending percentages of the response indicators compared with original system.

Indexes	The descending percentage of the maximum bodywork acceleration (%)	The descending percentage of the maximum bodywork travel (%)	The descending percentage of the maximum suspension travel (%)	The descending percentage of the maximum tire dynamic load (%)	The descending percentage of the maximum IWM's MMG (%)
Using parameters optimized by the GA	22	10	38	18	11
Using parameters optimized by the proposed method	28	18	74	39	53

It can be seen from Figures 9(a)–9(e) that the original nonlinear IWM-suspensions coupling system cannot attenuate vibration rapidly, while the GA-optimized and the proposed method-optimized coupling systems have vibration damping performance under bumpy road excitation. Compared with the GA-optimized nonlinear coupling system, the proposed method-optimized one can weaken vibration amplitudes quickly and has shorter time to reach steady state. The proposed AFSA-based optimization method can well suppress the vibration of nonlinear IWM-suspensions coupling system on bumpy road, simultaneously limit the suspension travel within its allowable range, and more effectively reduce the bodywork vertical vibration acceleration and amplitude. Therefore, the nonlinear IWM-suspensions coupling system optimized by the proposed method has better synthesized dynamic performance which indicates the proposed AFSA-based optimization method can well improve the ride comfort of electric wheel vehicle on bumpy road.

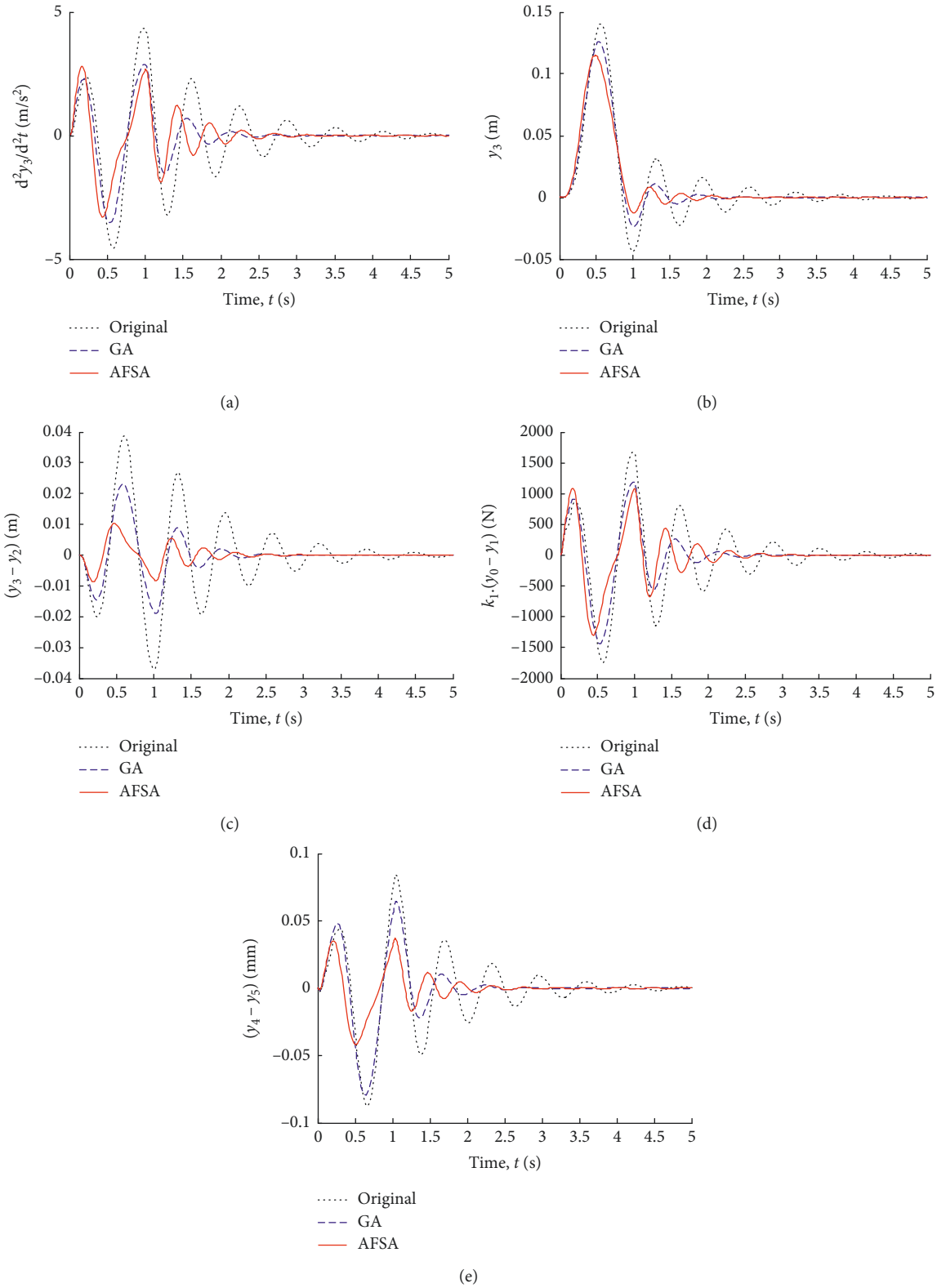

Figure 9: The response comparisons of the coupling system optimized by different methods. (a) The bodywork acceleration. (b) The bodywork travel. (c) The suspension travel. (d) The tire dynamic load. (e) The vertical MMG.

5. Conclusion

Based on the established novel dynamics model of nonlinear IWM-suspensions coupling system which includes the MMG of IWM, the AFSA-based multiobjective optimization mathematical model and method are proposed to optimize multiple dynamics parameters of the coupling system. Under rough and bump road excitations, numerical results show that the dynamic performances of the proposed method-optimized coupling system are well improved and the optimal dynamics parameter combinations are obtained. More importantly, by using the proposed optimization method, the MMG's vertical fluctuation and the bodywork vertical vibration acceleration can be effectively reduced which can decrease electromagnetic force waves and motor wear, extend bearing life, and significantly improve the ride comfort of electric wheel vehicle. Compared with the GA-optimized system and the original system without optimization, the system optimized by the proposed AFSA-based method has the best dynamic characteristics, which verifies the methodological optimization control effect, global convergence characteristic, and superiority than the GA under the same optimization conditions. The methodology investigated by this paper gives a valuable means to the optimization control of IWM-suspensions coupling system. As future work, it is beneficial to discuss the differences of different optimization methods, e.g., DE, PSO, the proposed AFSA-based method, and so on and study the parameter selection method of the proposed optimization algorithm so that we can improve the dynamic performance of IWM-suspensions coupling system further.

Data Availability

The source codes are given as supplementary materials named MATLAB.zip.

Conflicts of Interest

The authors declare no potential conflicts of interest with respect to the research, authorship, and/or publication of this article.

Acknowledgments

This study was funded by the National Key Research and Development Program of China (grant no. 2016YFD0700800) and the Shaanxi Province Key Research and Development Program of China (grant no. 2017NY-176). The authors would like to appreciate all the authors listed in the references and would also like to thank the funding organizations that provided financial support.

Supplementary Materials

The description of supplementary materials is "Matlab Codes of AFSA, GA, and Simulation." (*Supplementary Materials*)

References

[1] C. Pomponi, S. Scalzi, L. Pasquale, C. M. Verrelli, and R. Marino, "Automatic motor speed reference generators for cruise and lateral control of electric vehicles with in-wheel motors," *Control Engineering Practice*, vol. 79, pp. 126–143, 2018.

[2] X. Shao, F. Naghdy, H. Du, and Y. Qin, "Coupling effect between road excitation and an in-wheel switched reluctance motor on vehicle ride comfort and active suspension control," *Journal of Sound and Vibration*, vol. 443, pp. 683–702, 2019.

[3] L. Qin, Y. Yu, C. Zhou, S. Mao, and F. Yang, "Simulation of vertical characteristics and in-wheel motor vibration of electric vehicles with asymmetric suspension damper under road impact," *International Journal of Modelling and Simulation*, vol. 39, no. 1, pp. 14–20, 2019.

[4] Y. Mao, S. Zuo, X. Wu, and X. Duan, "High frequency vibration characteristics of electric wheel system under in-wheel motor torque ripple," *Journal of Sound and Vibration*, vol. 400, pp. 442–456, 2017.

[5] Y. Duan, P. Li, and G. Ren, "Electric vehicles with in-wheel switched reluctance motors: coupling effects between road excitation and the unbalanced radial force," *Journal of Sound and Vibration*, vol. 372, pp. 69–81, 2016.

[6] X. Zeng, G. Li, G. Yin, D. Song, S. Li, and N. Yang, "Model predictive control-based dynamic coordinate strategy for hydraulic hub-motor auxiliary system of a heavy commercial vehicle," *Mechanical Systems and Signal Processing*, vol. 101, pp. 97–120, 2018.

[7] X. Shao, F. Naghdy, and H. Du, "Reliable fuzzy H_∞ control for active suspension of in-wheel motor driven electric vehicles with dynamic damping," *Mechanical Systems and Signal Processing*, vol. 87, pp. 365–383, 2017.

[8] H. Pang, X. Zhang, and Z. Xu, "Adaptive backstepping-based tracking control design for nonlinear active suspension system with parameter uncertainties and safety constraints," *ISA Transactions*, vol. 88, pp. 23–36, 2019.

[9] A. C. Mitra, T. Soni, G. R. Kiranchand, S. Khan, and N. Banerjee, "Experimental design and optimization of vehicle suspension system," *Materials Today Proceedings*, vol. 2, no. 4-5, pp. 2453–2462, 2015.

[10] Z. Cheng and Z. Lu, "Research on the PID control of the ESP system of tractor based on improved AFSA and improved SA," *Computers and Electronics in Agriculture*, vol. 148, pp. 142–147, 2018.

[11] M. P. Nagarkar, Y. J. Bhalerao, G. J. V. Patil, and R. N. Z. Patil, "GA-based multi-objective optimization of active nonlinear quarter car suspension system—PID and fuzzy logic control," *International Journal of Mechanical and Materials Engineering*, vol. 13, no. 1, pp. 1–20, 2018.

[12] A. C. Mitra, G. J. Desai, S. R. Patwardhan, P. H. Shirke, W. M. H. Waseem, and N. Banerjee, "Optimization of passive vehicle suspension system by genetic algorithm," *Procedia Engineering*, vol. 144, pp. 1158–1166, 2016.

[13] M. B. S. S. Reddy, P. Vigneshwar, M. S. Ram, D. R. Sekhar, and Y. S. Harish, "Comparative optimization study on vehicle suspension parameters for rider comfort based on RSM and GA," *Materials Today: Proceedings*, vol. 4, no. 2, pp. 1794–1803, 2017.

[14] Y. Wang, W. Zhao, G. Zhou, Q. Gao, and C. Wang, "Optimization of an auxetic jounce bumper based on Gaussian process metamodel and series hybrid GA-SQP algorithm," *Structural and Multidisciplinary Optimization*, vol. 57, no. 6, pp. 2515–2525, 2018.

[15] B. Gadhvi, V. Savsani, and V. Patel, "Multi-objective optimization of vehicle passive suspension system using NSGA-II, SPEA2 and PESA-II," *Procedia Technology*, vol. 23, pp. 361–368, 2016.

[16] X. Ma, P. K. Wong, and J. Zhao, "Practical multi-objective control for automotive semi-active suspension system with nonlinear hydraulic adjustable damper," *Mechanical Systems and Signal Processing*, vol. 117, pp. 667–688, 2019.

[17] F. Bianchini, "Artificial intelligence and synthetic biology: a tri-temporal contribution," *Biosystems*, vol. 148, pp. 32–39, 2016.

[18] K. Chakkarapani, T. Thangavelu, K. Dharmalingam, and P. Thandavarayan, "Multi objective design optimization and analysis of magnetic flux distribution for slotless permanent magnet brushless DC motor using evolutionary algorithms," *Journal of Magnetism and Magnetic Materials*, vol. 476, pp. 524–537, 2019.

[19] I. Rahman and J. Mohamad-Saleh, "Plug-in electric vehicle charging optimization using bio-inspired computational intelligence methods," in *Sustainable Interdependent Networks*, vol. 145, pp. 135–147, Springer, Berlin, Germany, 2018.

[20] J. He, X. Jin, S. Y. Xie, L. Cao, Y. Lin, and N. Wang, "Multi-body dynamics modeling and TMD optimization based on the improved AFSA for floating wind turbines," *Renewable Energy*, vol. 141, pp. 305–321, 2019.

[21] K. P. Kumar, B. Saravanan, and K. S. Swarup, "Optimization of renewable energy sources in a microgrid using artificial fish swarm algorithm," *Energy Procedia*, vol. 90, pp. 107–113, 2016.

[22] Z. Zhang, K. Wang, L. Zhu, and Y. Wang, "A pareto improved artificial fish swarm algorithm for solving a multi-objective fuzzy disassembly line balancing problem," *Expert Systems with Applications*, vol. 86, pp. 165–176, 2017.

[23] Y.-Z. Wang, Z.-W. Li, Y.-X. Kou, Q.-P. Sun, H.-Y. Yang, and Z.-Y. Zhao, "A new approach to weapon-target assignment in cooperative air combat," *Mathematical Problems in Engineering*, vol. 2017, Article ID 2936279, 17 pages, 2017.

[24] H. Pan, X. Jing, and W. Sun, "Robust finite-time tracking control for nonlinear suspension systems via disturbance compensation," *Mechanical Systems and Signal Processing*, vol. 88, pp. 49–61, 2017.

[25] Z. Gao, S. Chen, Y. Zhao, and Z. Liu, "Numerical evaluation of compatibility between comfort and energy recovery based on energy flow mechanism inside electromagnetic active suspension," *Energy*, vol. 170, pp. 521–536, 2019.

[26] W. Liu, Y. L. Song, J. Chen, and S. Shi, "A novel optimal fuzzy integrated control method of active suspension system," *Journal of the Brazilian Society of Mechanical Sciences and Engineering*, vol. 40, no. 1, p. 29, 2018.

[27] D. Y. Zhuang, K. Ma, C. A. Tang, Z. Z. Liang, K. K. Wang, and Z. W. Wang, "Mechanical parameter inversion in tunnel engineering using support vector regression optimized by multi-strategy artificial fish swarm algorithm," *Tunnelling and Underground Space Technology*, vol. 83, pp. 425–436, 2019.

[28] Y. Luo and D. Tan, "Study on the dynamics of the in-wheel motor system," *IEEE Transactions on Vehicular Technology*, vol. 61, no. 8, pp. 3510–3517, 2012.